Low-frequency tremor and slow slip around the probable source region of the Tokai Earthquake – A new indicator for the Tokai Earthquake prediction provided by unified seismic networks in Japan –

Noriko Kamaya (Seismological and Volcanological Department, JMA),
Akio Katsumata (Meteorological College, JMA)
and
Yuzo Ishigaki (Seismological and Volcanological Department, JMA)

Abstract

Enhancement of seismic networks in the Japan Islands of these years revealed occurrence of deep low-frequency continuous tremors of a belt distribution in the southwest Japan, where the subducting Philippine Sea plate reaches depths of 25–40 km. The source region of the tremor is assumed to correspond to boundary region between oceanic and island crusts close to mantle wedge. The east end of the belt tremor distribution is adjacent to the probable source region of the Tokai Earthquake. A slow-slip event has continued in the west of the source region of the Tokai Earthquake since 2000. Synchronous activation of the tremor and slow-slip speed was observed in 2003. This suggests some relationship between the slow-slip and the tremor activity. We expect that the tremor activity could be a new valuable indicator for the Tokai Earthquake prediction. The long duration of the tremor indicates existence of fluid relating to its generation. The most probable fluid is considered to be water produced by dehydration of chlorite and formation of clinopyroxene in the oceanic crust on the basis of data from high pressure and temperature experiments. The northern border of the belt distribution is possibly rimmed by the edge of the mantle wedge because serpentine formation absorbs fluid water.

1 Introduction

Since Oct. 1997, short-period seismic records obtained at most of stations in the Japan Islands have been transmitted to the Japan Meteorological Agency (JMA). The JMA has processed those records to make a comprehensive seismic catalog in Japan. The short-period instruments include those installed by universities, the National Research Institute for Earth Science and Disaster Prevention (NIED), the JMA, other national institutes, and local governments. This integrated processing lowered the detectable magnitude of earthquakes. Moreover, deployment of the Hi-net [e.g., *Okada et al.*, 2000], which is a dense network of highly sensitive short-period instruments installed by the NIED, improved the detectivity remarkably. Hi-net data has been included to produce the seismic catalog since Oct. 2000.

Fig. 1 shows stations which contribute the current unified seismic catalog. Seven cable-type ocean-bottom seismometry systems are included in the network.

Fig. 2 shows magnitude-time distribution since 1965. The magnitudes are determined from maximum displacement or velocity amplitudes [*Tsuboi* , 1954; *Katsumata*, 2004; *Funasaki et al.*, 2004]. It is recognized that the lowermost magnitude has continued to decrease year by year since 1970s. More than 130,000 hypocenters are located in and around the Japanese Islands in 2003. Fig. 3 shows numbers of hypocenter determinations in a year in the JMA (1926–Sep. 1997) and the unified (Oct. 1997–) seismic catalogs. A level of one thousand a year had continued until mid of 1970s. Since then, introductions of high-sensitive seismometers, automated digital processing systems and densely distributed seismic networks have increased the number of located hypocenters.

The enhanced detection ability revealed occurrence of low-frequency microearthquakes at depths of 20–40km in the Japan Islands. The JMA has distinguished those deep low-frequency earthquakes in the seismic catalog since Oct. 1999. The deep low-frequency earthquakes are indicated by red symbols in Fig. 2. Magnitude of most of those events are less than magnitude 2.0, and many of those are less magnitude 1.0. Occur-

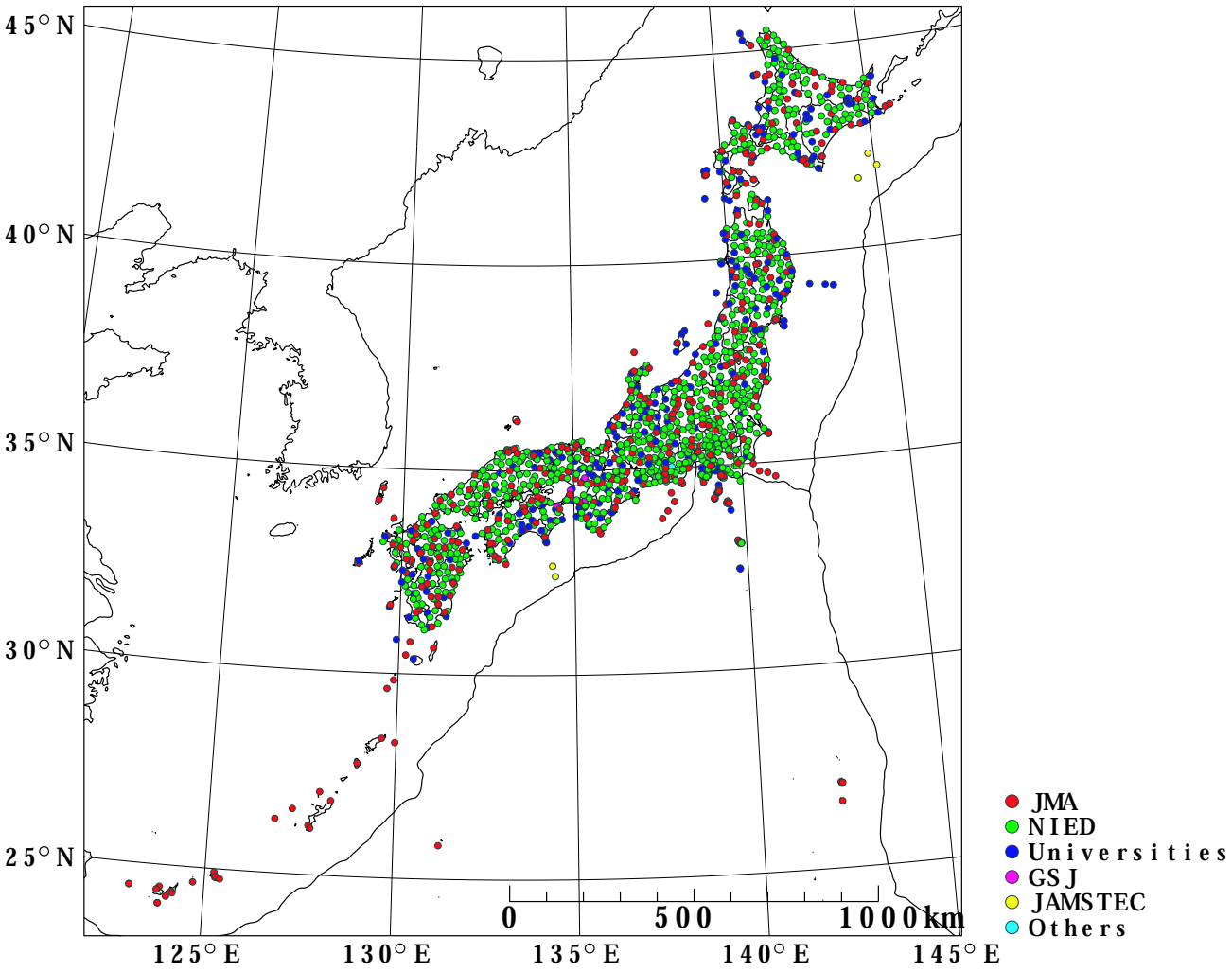

Figure 1: Stations which contribute the current unified seismic catalog.

rence of low-frequency events around the Moho discontinuity in the areas away from volcanoes became recognized based on the seismic catalog [*Nishide et al.*, 2000]. Although seismicity of low-frequency events beneath volcanoes has been well-known [e.g., *Hasegawa et al.*, 1991; *Hasegawa and Yamamoto*, 1994; *Ukawa and Obara*, 1993], seismic activities away from volcanic areas had not been noticed.

Nishide et al. (2000) recognized low-frequency seismic activities in the east of Aichi Prefecture (34.8° ∼ 35.3°N, 137° ∼ 138°E. See Fig. 8), which was recognized as a part of belt distribution of deep low-frequency tremor along the strike of the subducting Philippine Sea plate [*Obara*, 2002; *Katsumata and Kamaya*, 2003] after deployment of the Hi-net.

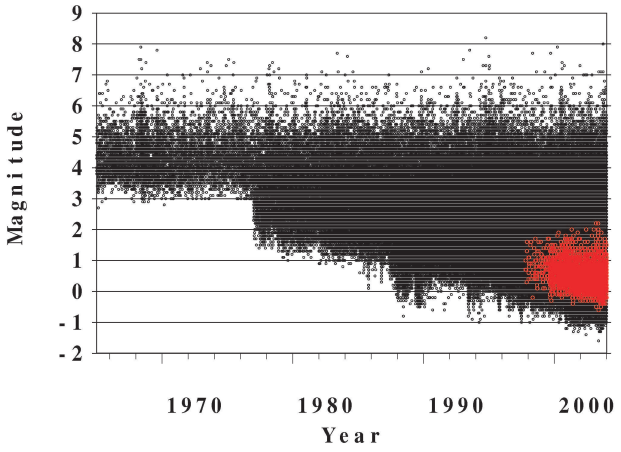

Figure 2: Magnitude-time distribution since 1965 in the JMA and the unified seismic catalogs. Red small circles denote the events labeled as the deep low-frequency earthquakes.

The deep low-frequency tremor (LFT in this article) is the most notable phenomena which was found by the recently deployed dense seismic network. We describe the activity of the deep tremor, and discuss its source characteristics in this article. In addition to the deep tremor, low-frequency earthquakes around the Moho discontinuity were found not only in volcanic regions but also in non-volcanic areas. We use a term of deep low-frequency earthquake (LFE in this article) to describe such activities.

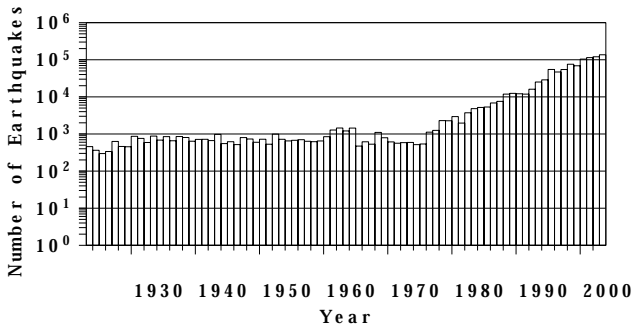

Figure 3: Number of earthquakes listed in the JMA (1926–Sep. 1997) and the unified (Oct. 1997–) seismic catalogs.

2 Seismicity of Deep Low-Frequency Tremors and Earthquakes

In this section, we describe spacial and temporal characteristics of the LFT in the southwest Japan. Activities of LFE in volcanic and non-volcanic regions are also explained.

2.1 Source Locations of Deep Low-Frequency Tremors in the Southwest Japan

The JMA estimates the source locations of LFT by an ordinary hypocenter determination method based on the onset times of enlarging parts of the tremors. This is different from the method of *Obara* (2002) who estimated the locations of LFT by applying S-wave velocity model to envelopes of tremor waveforms. Fig. 4 shows examples of the observed tremor waveforms. Broken curves in the figure denote calculated arrival times based on locations estimated by the JMA. Onsets of the tremor are close to the calculated S travel times. Corresponding onsets of P-waves are seldom seen even on the vertical component. Lack of P-wave arrival data makes accuracy of source depths poor.

Although most of LFT do not show onsets of P-wave, a small number of LFT segments do show onsets of P-wave. Depth of those events are rather precise. Fig. 5 shows an epicenter map and a cross section of the deep low-frequency events with relatively small estimation errors in the southwest Japan. In the figure, orange circles show events occurring within 10 km (epicentral distance) from the centers of volcanoes which have been active in the Quaternary [*Committee for Catalog of Quaternary Volcanoes in Japan*, 1999], and blue circles show events away from volcanoes. The estimated depths of the most of non-volcanic events were distributed from 25 to 40 km. and the average depth is about 30 km.

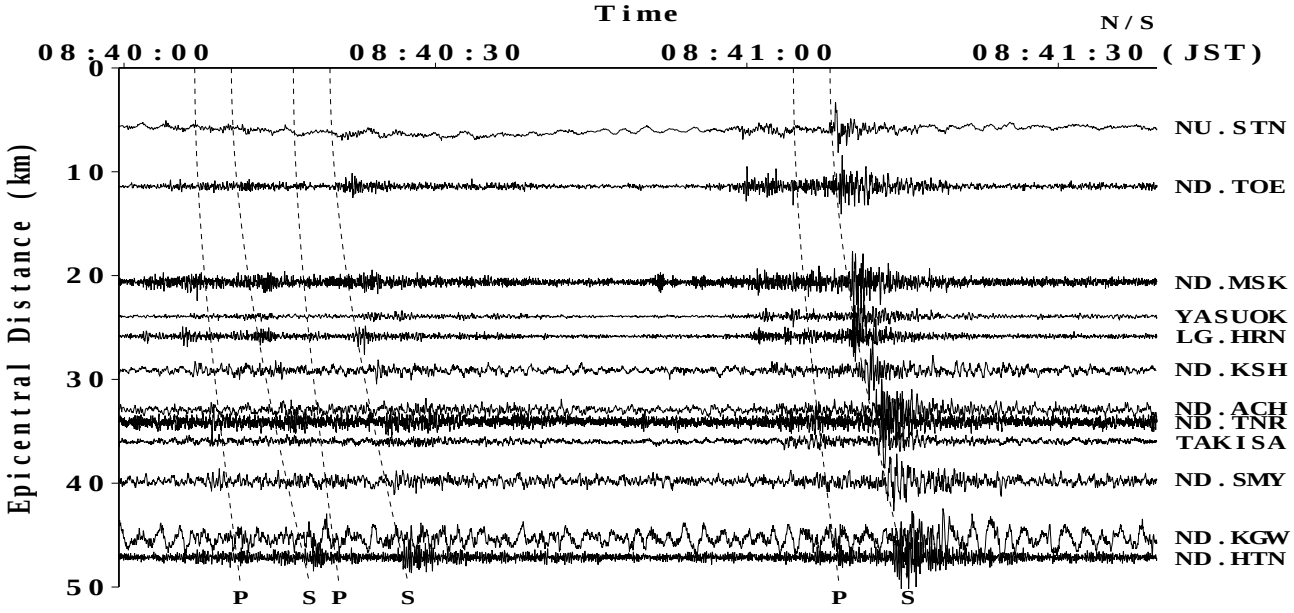

Figure 4: Example of LFT observed on June 3, 2001. Waveforms are arranged in epicentral distance order from an estimated source location. Broken lines show calculated P and S travel times for enlarging parts of the tremor. Station code are denoted on the right side. ND, NU, and LG signify the NIED, Nagoya University, and local government, respectively. YASUOK and TAKASA are stations of the JMA.

Fig. 6 show source locations of LFT (blue circles) from September, 1999 to September, 2001 beneath eastern Shikoku (133.6° – 134.5°E) projected onto the vertical structural cross-section from *Kurashimo et al.* (2002), which is based on seismic velocities. The LFT are located in boundary region between oceanic and island crusts close to the mantle wedge. It is notable that the LFT are not distributed boundary regions between oceanic crust and mantle wedge.

2.2 Temporal Characteristics of the Deep Low-Frequency Tremor Activities

Fig. 7 (b) shows time-space distribution of LFT. Most event show episodic activity. Active period continues for several hours – several days.

Fig. 7 (c) and (d) show accumulated numbers of events and quiescent periods of the tremor activities in partitioned areas shown in (b). The quiescent period in the figure is defined as a time interval without any detected tremor events more than two days.

It is recognized from Fig. 7 (b) and (c) that the tremor activities are not stationary. Accumulated numbers and quiescent periods changes with some trends.

In the region (2) (Fig. 7 (b)), shortening of quiescent periods started late in 2002. Short quiescent periods have been kept for about half year from the 4th quarter of 2003 to the 1st quarter of 2004. Then quiescent periods were prolonged in 2004, but they are still short compared with the average in 2002. The period of 2003–2004 corresponds to periods of relatively fast slow-slip in Tokai area, which is discussed in a latter section.

In the region (4), short quiescent periods have been kept since middle of 2004. It seems that there has been some activity in the region.

In the regions (8), (9) and (10), shortening of quiescent periods appear relatively regularly. It takes about a few months from starting of shortening to returning to regular quiescent period of about several tens of days.

In the regions (11) and (12), state of short quiescent periods was kept for a few months in 2003. The shortening started from the beginning of 2003, and prolonging had continued until beginning of 2004. Slow-slip events were observed in the period by *Hirose and Obara* (2003) in the region. The graph of accumulated number of events also show a unusual rate in the period.

The activity of LFT should indicate some state of plate coupling. But its mechanism is to be investigated.

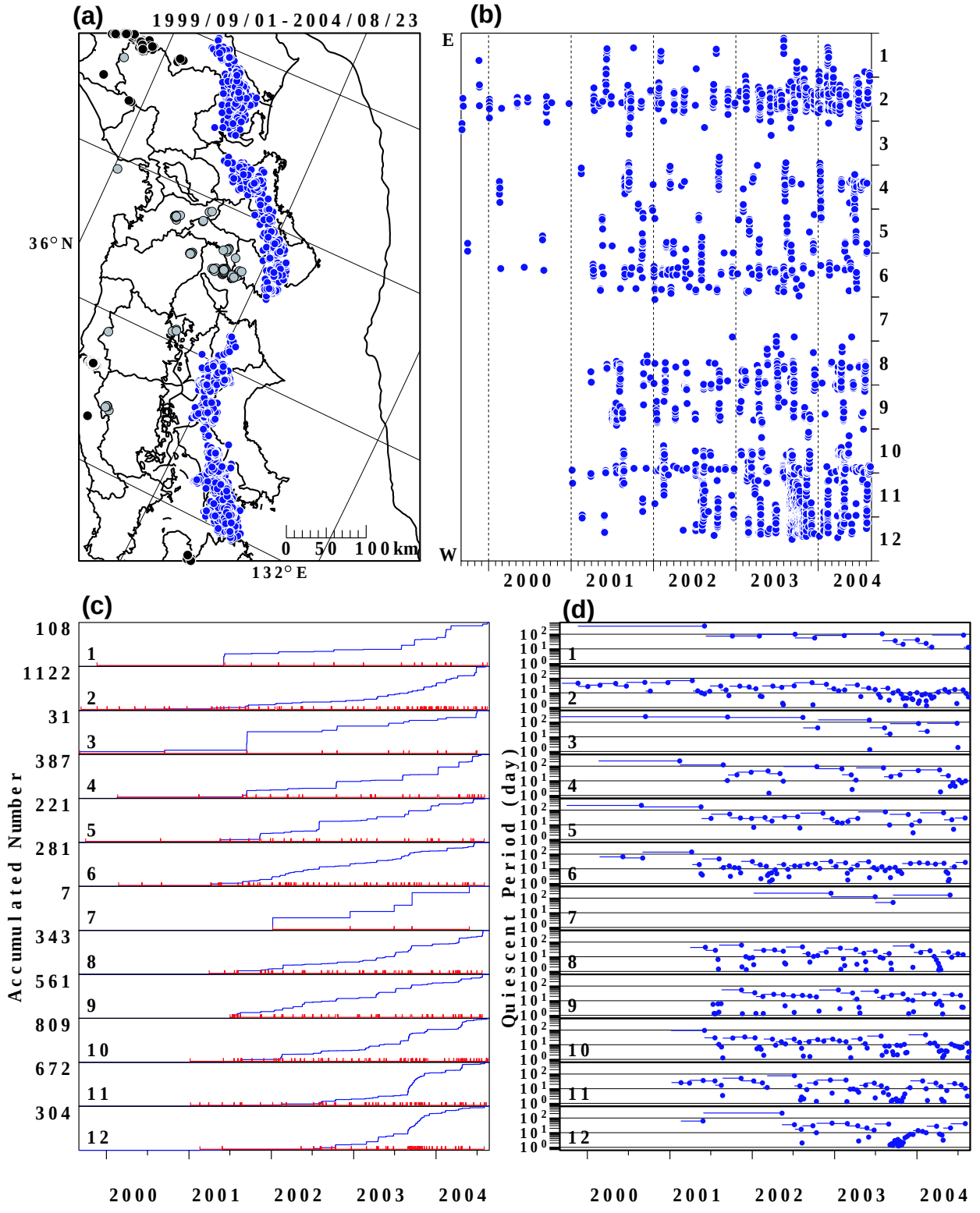

Figure 7: Temporal variation of the deep low-frequency tremor activities. (a) Epicenter map; (b) time-space distribution; (c) accumulated number; (d) quiescent period. Accumulated number of events and quiescent period are shown for regions of which numbers are denoted on the right of (b).

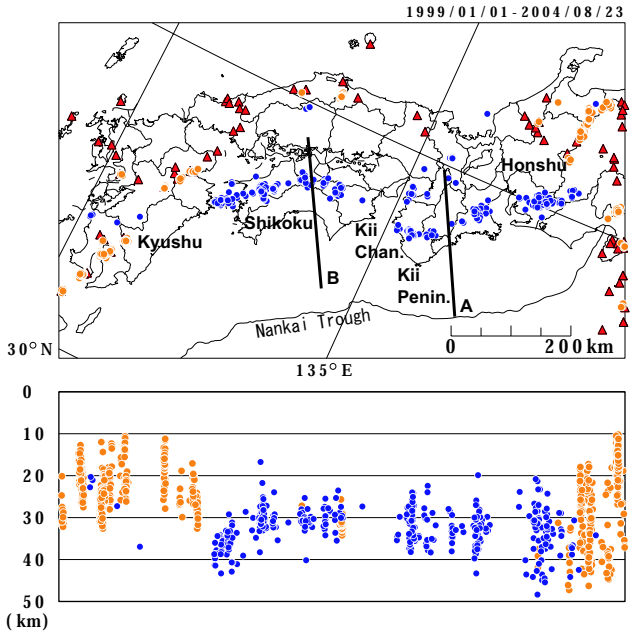

Figure 5: Distribution of LFT and LFE in the southwest Japan (Jan. 1999 – Aug. 2004). Blue circles, orange ones and red triangles show source locations of non-volcanic LFE and LFT, LFE close to volcanoes, and active volcanoes in the Quaternary, respectively. The line segments A and B indicate Tonankai and Nankaido profiles for which *Hyndman et al.* (1995) estimated geotherms, respectively.

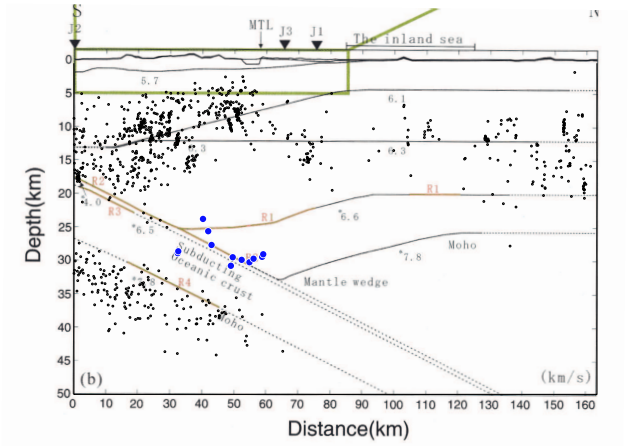

Figure 6: Source locations of LFT (blue circles) from September, 1999 to September, 2001 beneath eastern Shikoku (133.6° – 134.5°E) projected onto the vertical structural cross-section from *Kurashimo et al.* (2002), which is based on seismic velocities. The horizontal axis represents the distance from shot J2 of *Kurashimo, et al.* (2002) which was located near the south coast of Shikoku Island. Black dots denote ordinary earthquakes.

2.3 Deep Low-Frequency Earthquakes in the Northeast Japan

Deep low-frequency earthquakes have been found in wide area in the Japan Islands [*Kamaya and Katsumata*, 2004]. Fig. 8 shows epicenters of the LFE. Orange circles show LFE occurring within 10 km (epicentral distance) from the centers of volcanoes which have been active in the Quaternary [*Committee for Catalog of Quaternary Volcanoes in Japan*, 1999], and blue circles show LFE away from volcanoes which include LFT. The estimated depths of the most of non-volcanic events were distributed from 25 to 40 km, and the average depth is about 30 km. Active volcanoes and the Quaternary volcanoes are shown by red triangles. In the figure, contours show the tops of the Pacific and the Philippine Sea plates which were estimated as upper limits of seismicity in the plate.

LFE in the northeast Japan are distributed only in the back-arc side of the volcanic front which is almost coincides with a 110 km depth contour of the Pacific plate. There is no activities in the fore-arc side of the volcanic front. The distribution indicates the LFE in the northeast Japan are related to volcanic activity even in the cases away from volcanoes. If we include regions with igneous rocks in the Tertiaries, all LFE-active regions in the northwest Japan are covered.

2.4 Deep Low-Frequency Earthquakes in the Southwest Japan

In addition to deep low-frequency tremor activities, there are some spot distributions of LFE in the southwest Japan (gray-filled circles in Fig. 7 (a)). Some of those clusters are distributed along the volcanic front of the Philippine Sea plate. But some clusters are distributed in fore-arc side of the volcanic front (clusters in 133°–136°E and 35.1°–35.7°N).

Fig. 9 (a) and (d) show waveform and spectrum of a horizontal (NS) component from a low-frequency earthquake obtained at a station in Tannan (DP.TNJ, 35.0313°N, 135.2137°E) for an event which occurred in Kyoto Pref. (hypocenter: 35.1185°N, 135.5775°E, 34.7km) at 01:41:41.1, July 30 2000 JST. Waveforms of events in this region usually show a clear onsets and long duration. This is similar to waveforms of LFE in volcanic regions.

The bold spectrum curve corresponds to the 30s waveform segment indicated by the bold line in the waveform. The thin spectrum curve corresponds to the noise level as calculated for the 30s

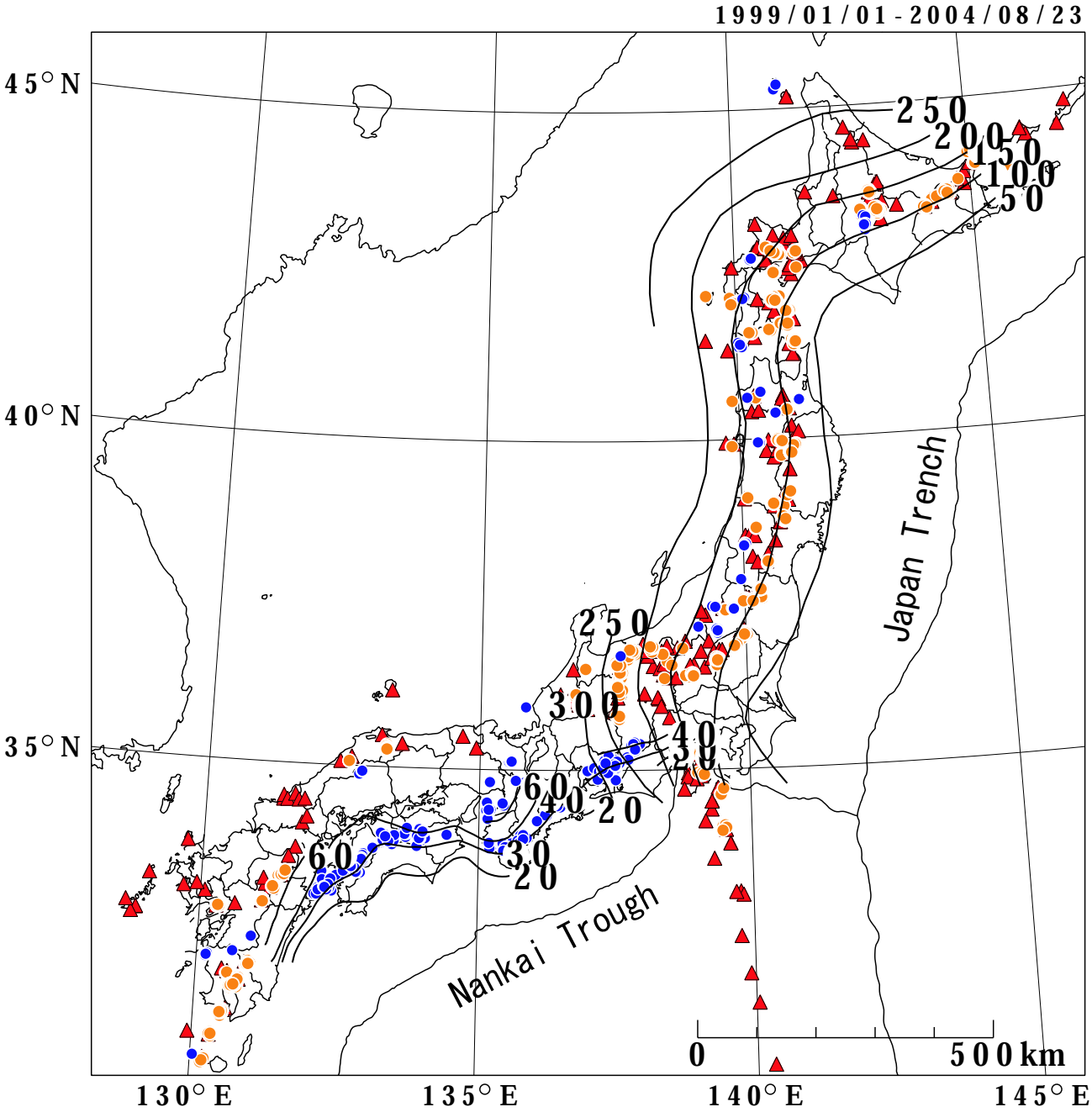

Figure 8: Distribution of epicenters of low-frequency events near the Mohorovicic discontinuity under the Japan Islands as determined by the Japan Meteorological Agency (JMA) from September, 1999 to August 23, 2004. Orange circles show events within 10km of active volcanoes and volcanoes which have been active in the Quaternary [*Committee for catalog of Quaternary volcanoes in Japan*, 1999], and blue circles show events away from those volcanoes. Active volcanoes and the Quaternary volcanoes are shown by red triangles. Also shown are parts of depth contours for the upper surfaces of the Pacific Plate and the Philippine Sea Plate. The contours are labeled with depth in km.

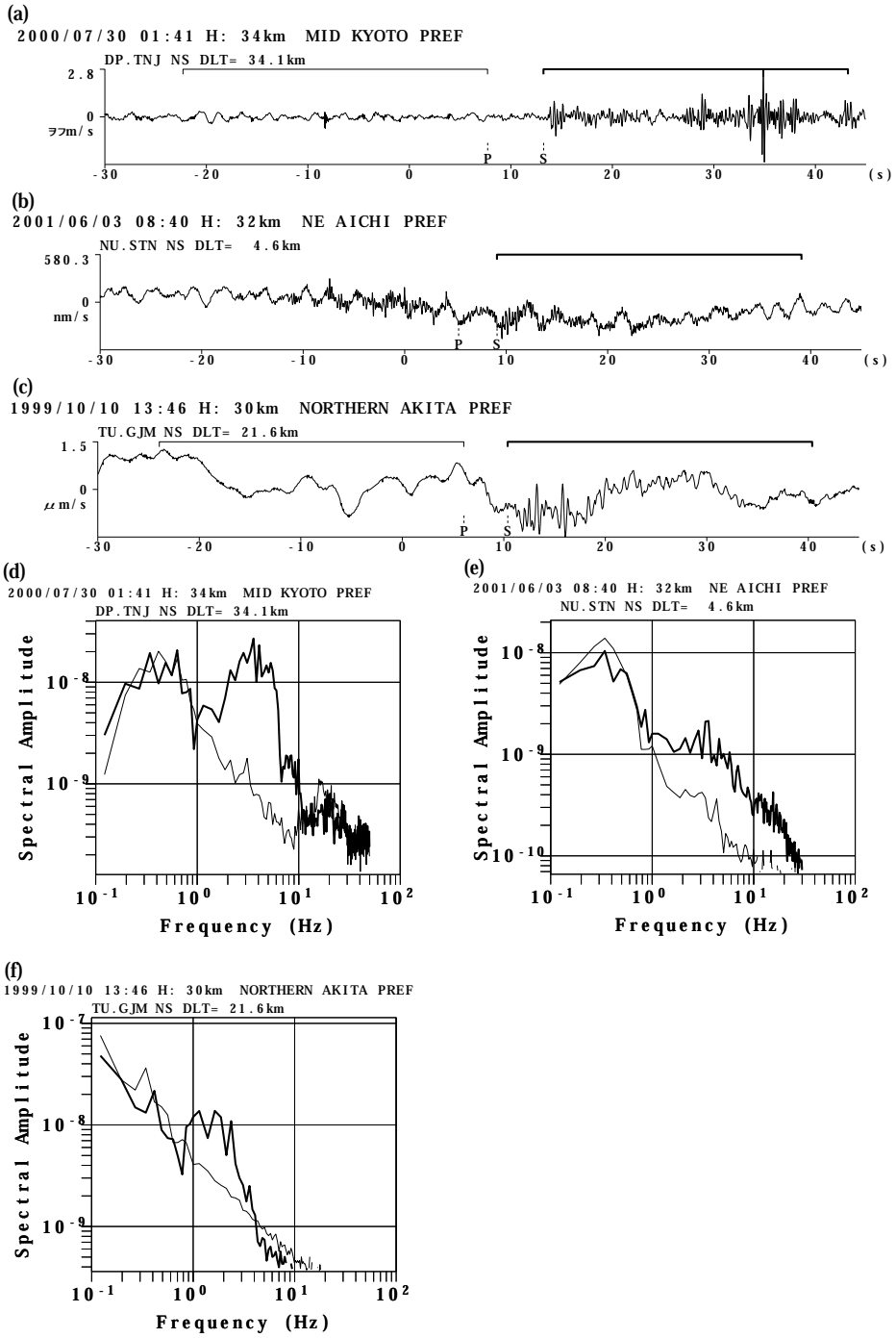

Figure 9: Spectra of deep low-frequency events in the Japan Islands. a) and d) A waveform and its spectrum of horizontal (NS) component from a low-frequency earthquake obtained at a station in Tannan (DP.TNJ, 35.0313N, 135.2137E) for an event which occurred in Kyoto Pref. at 01:41:41.1, July 30 2000. The bold spectrum curve corresponds to the 30s waveform segment indicated by the bold line in the waveform. The thin spectrum curve corresponds to the noise level as calculated for the 30s waveform segment indicated by the thin line in the waveform. H and DLT denote the focal depth and epicentral distance. b), c), e) and f) show waveforms and spectra for a low-frequency tremor in southwestern Japan and a low-frequency earthquake away from volcanoes in northeastern Japan, respectively. The records were obtained at Shin-Toyone (NU.STN, 35.1355N, 137.7437E) and Gojome (TU.GJM, 39.9520N, 140.1160E).

waveform segment indicated by the thin line in the waveform. The seismic wave from the event has power in the frequency rage of 1–10 Hz. (b), (c), (e) and (f) in Fig. 9 show waveforms and spectra for a low-frequency tremor in southwestern Japan and a low-frequency earthquake away from volcanoes in northeastern Japan, respectively. The spectra of these events do not show no effective spectral contents in a frequency range lower than 1 Hz. It is interesting that the deep tremor and LFE has common characteristics in spectrum.

3 Tokai Slow-Slip and the Tremor

A great earthquake is expected to occur along the Suruga Trough where the Philippine Sea plate subducts beneath the Eurasian plate. The earthquake is named Tokai Earthquake prior to its occurrence. Fig. 10 shows the probable source region of the Tokai Earthquake.

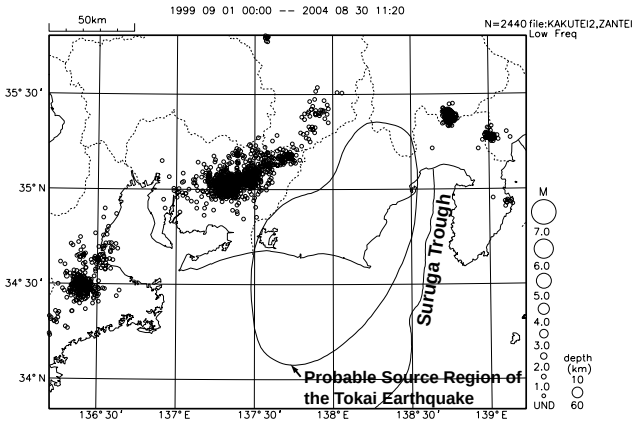

Figure 10: Probable source region of the Tokai Earthquake and epicenters of deep low-frequency events.

In the west of the probable source area, slow-slip events has been observed since 2000. Fig. 11 shows the vertical displacement measured by GEONET, GPS Earth Observation Network of the Geographical Survey Institute of Japan. Fig. 12 shows temporal variation of crustal deformation observed at Hamakita GEONET station.

Relatively high-speed deformation is seen in 2003–2004 in Fig. 12. Active state of the deep tremor has been continuing in the northwest region of the slow-slip area since 2003 (the region 2 in Fig. 7). The fast crustal deformation in 2003–2004 is simultaneous with the abnormal tremor activity since 2003. We suspect that there would be some interactions between the slow-slip and deep tremor activity. We consider that the deep tremor activity would be a indicator of some status of the coupling between the plates.

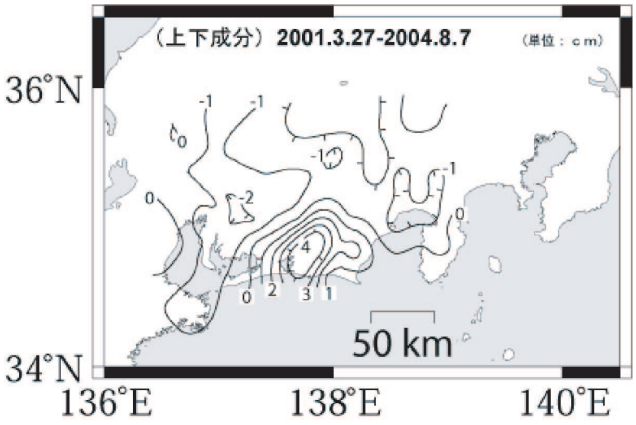

Figure 11: Vertical component of crustal deformation due to the Tokai slow-slip observed by the GEONET, GPS Earth Observation Network of the Geographical Survey Institute.

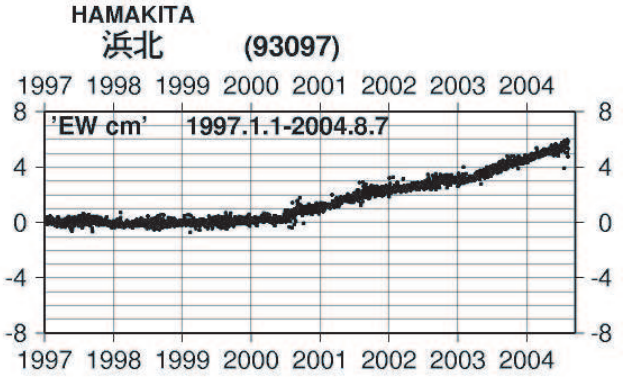

Figure 12: Temporal variation of location of the Hamakita GEONET station.

4 Source Characteristics of LFT

4.1 Source Force Direction of LFT

It is important to know the source mechanism of the tremor to understand this phenomena. S-wave is dominant on the tremor waveforms. It is considered that some kind of shear force causes the tremor.

We estimate source-force direction from particle motions of S-waves with a method by *Ukawa and Ohtake* (1987). We get S-wave polarization directions from particle motions of every two seconds with overlapping of one second as shown in Fig. 13. Lower panel in Fig. 13 show particle motions on radial-transverse (R-T), vertical-radial (Z-R)

and vertical-transverse (Z-T) planes. Polarization data indicated by circles on the upper-right corners of the chart of particle motions are used to estimate source mechanism.

We estimate source force directions for time-intervals with enough number of polarization data. Source force directions were estimated for single-force and double-couples models. Fig. 14 shows an example of a solution. Red line segments show observed polarization directions, and color map show residual distribution. Region of small residual is rather concentrated. This indicates that this kind of analysis can bring out informations on the tremor source mechanism.

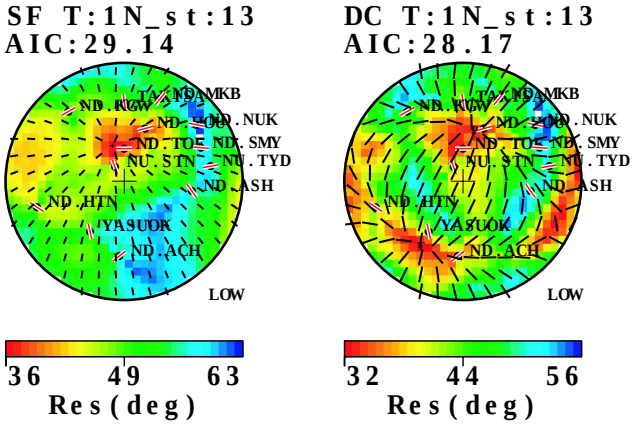

Figure 14: Source force directions inferred from particle motions for single-force (SF) and double-couples (DC) models projected on lower hemispheres.

Inferred P/T axes or force directions are shown in Figs. 15 (double-couple mode) and 16 (single force model), respectively. In this analysis, P/T axes are not distinguished because initial motion polarities are not used. Solutions of single force (Fig. 16) show relatively clear foci than those for double couple model. Source force directions of the tremor are distributed along NW-SE direction which is parallel to the direction of the Philippine Sea plate motion. This indicates that the motion of the Philippine Sea plate related to the tremor activities.

On the other hand, many of source-force directions of events around Mt. Fuji (138.7°E, 35.3°N) are nearly vertical. Those of events in the western Tottori area (around 133.3°E, 35.3°N) show similar tendency. Source-force direction of the tremor is clearly different from that of LFE in volcanic areas.

It is also notable that non-volcanic LFE in southwest Japan around 135°E, 35°N show similar

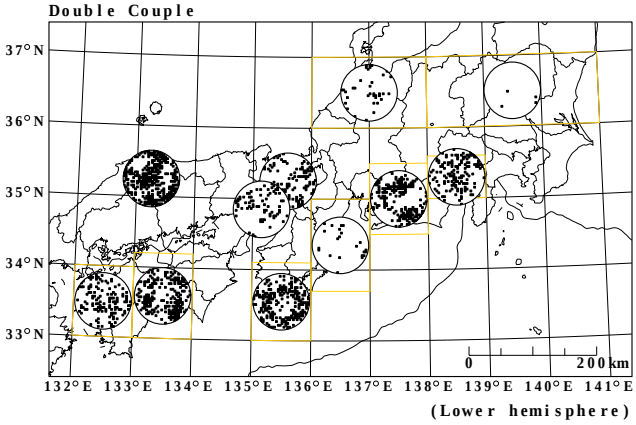

Figure 15: Inferred P- or T-axes for a double-couple model projected on a lower hemisphere of each region. Regions are shown with yellow rectangles.

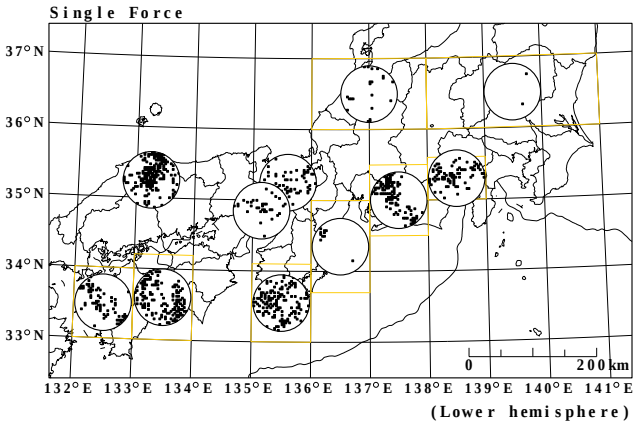

Figure 16: Inferred force direction for a single-force model projected on a lower hemisphere of each region. Regions are shown with yellow rectangles.

distribution as those in volcanic LFE. Although the region is in the fore-arc side of the volcanic front and in non-volcanic areas, the mechanism of LFE in the region would be similar to that in volcanic regions.

4.2 Source Spectrum of the Tremor

It is well-known that LFT show peak spectrum around 2–3 Hz. Fig. 17 shows an example of spectrum of the tremor. The spectrum is calculated directly from ground velocity record obtained with a broadband instruments (STS-1) without instrumental response correction. The black bold and blue thin curves show spectra of tremor-active period and period without tremor, respectively. Spectrum level is clearly different in a frequency range of 1–10 Hz. But no clear difference is seen in other frequency ranges. In the frequency range of 0.1–1 Hz, high-level ground noise due to micro-

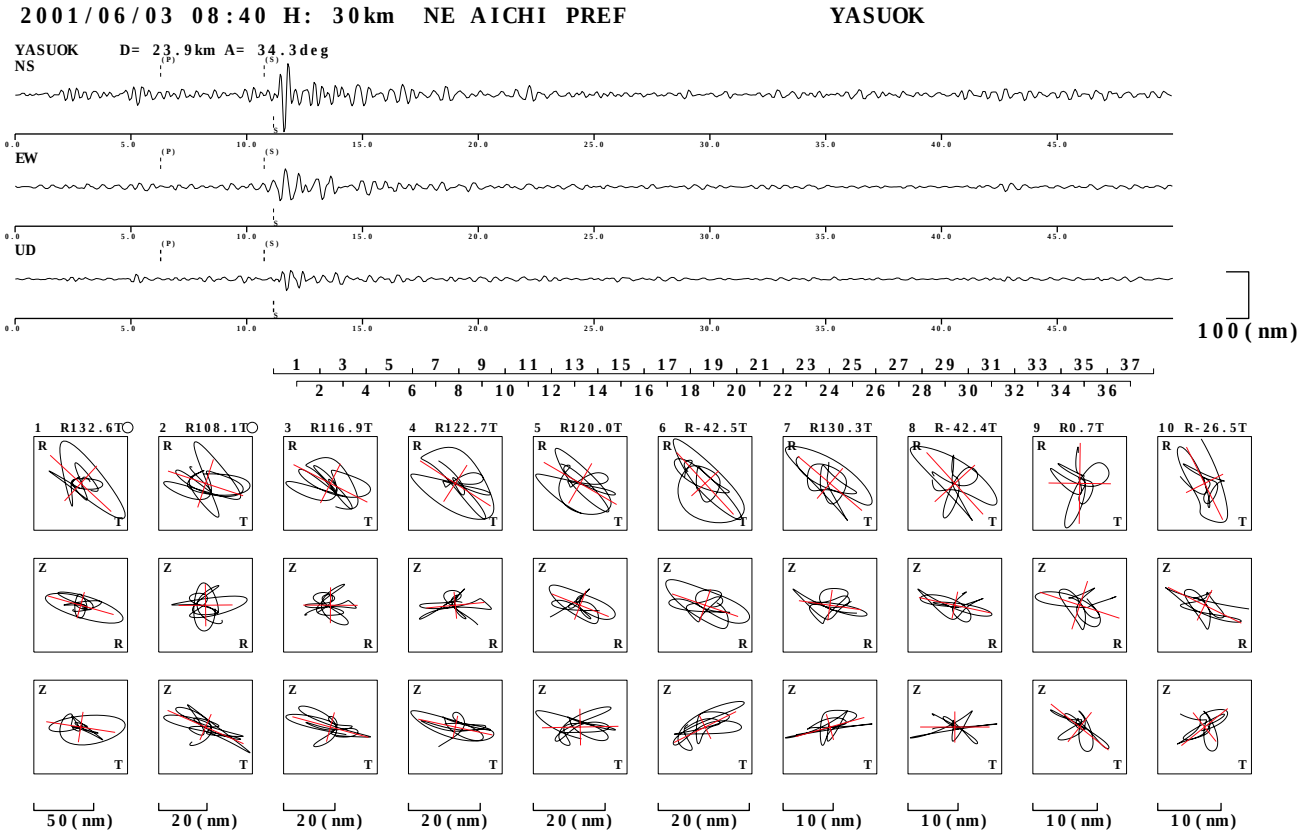

Figure 13: Particle motions of the tremor. The upper panel shows waveforms of three components, and the lower panel shows particle motions on radial-transverse (R-T), vertical-radial (Z-R) and vertical-transverse (Z-T) planes of every two second period with overlapping of one second.

seisms is recognized. In the range of 0.01–0.1 Hz in which the ground noise is low enough, power of the tremor is not recognized.

Hirose and Obara (2003) found slow-slip events simultaneous with deep tremor activities. If tremor is directly due to a slow-slip event, spectrum level at low frequency is higher than that at high frequency based on source spectrum models [e.g., *Aki*, 1967]. But no power is observed at frequency ranges of 0.01-0.1Hz. This indicates that there would be different power source for the tremor from the slow-slip.

5 Fluid Generation in the Tremor Source Region

The continuous tremors remind us of volcanic tremors, which are caused by some kinds of fluid [e.g., *Chouet*, 1996]. Deformation of ductile material may also show long duration like tremor.

Since a large quantity of water is conveyed by subduction of the Philippine Sea plate, water would be related to the deep tremor, directly or indirectly. Water would alter physical properties of minerals, and may cause tremor directly by moving or vibration.

We assume some possible sources of the water which is related to the deep tremor.

1. Extraction of interstitial water from oceanic crust.

2. Dehydration from minerals in the oceanic crust.

3. Dehydration from minerals in the mantle of the Philippine Sea plate.

4. Dehydration from minerals in the mantle wedge.

Although extraction of interstitial water from the oceanic crust might be a possible source, it would be difficult to explain why the extraction occurs at the restricted depth range of 25–40km. Since extraction of interstitial water should occur gradually, the limited depth range of water supply is considered to be related to limited pressure and temperature condition.

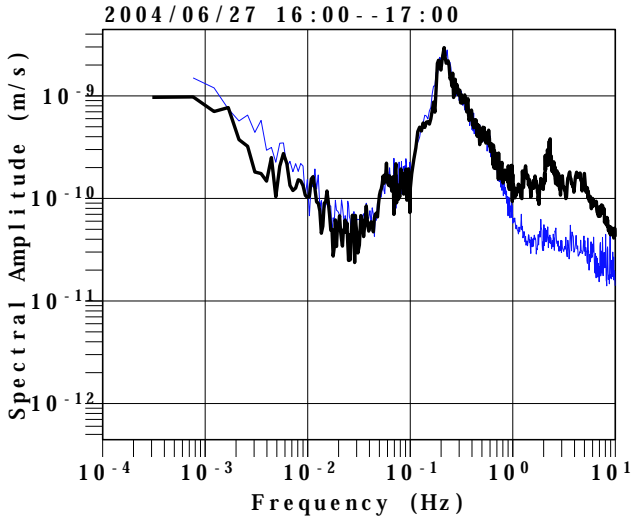

Figure 17: Spectrum of LFT observed at Asahi station (Fig. 18) of the F-net installed by the NIED. The black bold and blue thin curves show spectra of tremor-active period and period without tremor, respectively.

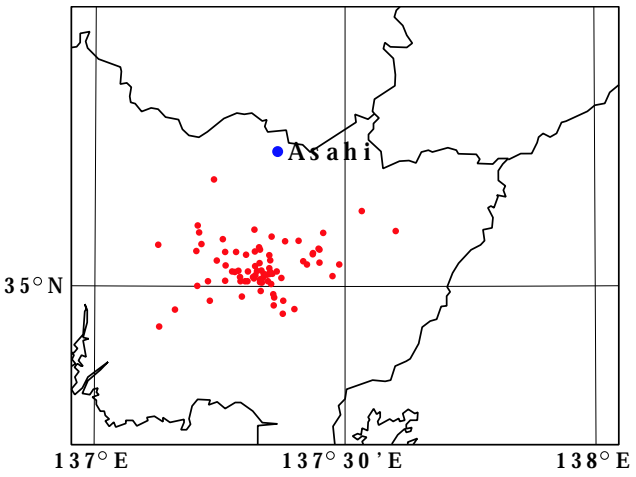

Figure 18: Station of Asahi (F-net of the NIED) and epicenters of LFT in June 2004 (red circles).

Fig. 19 shows the phase relationships for water-saturated mid-ocean ridge basalt obtained by *Schmidt and Poli* (1998). This phase relationships are applicable to minerals in a oceanic crust in a subducting slab. The broken curves in the figure show geotherms at the top of the subducting Philippine Sea plate estimated by *Hyndman et al.* (1995) for Tonankai and Nankaido profiles, respectively (Fig. 5). Depth contours in Fig. 8 were used to convert distance from the trench axis into depth at the top of the slab. The Philippine Sea plate subducts with a steeper incline beneath Kii Peninsula than beneath Shikoku. The geotherms cross the phase boundary shown by the heavy solid curve. Because chlorite can not exist in the region to the right of line "A", water is released by dehydration of chlorite along this line.

On the other hand, the temperature profile beneath Kii Peninsula crosses a thick line "B" at similar depth. Crossing this line, clinopyroxene appears. Because clinopyroxene is not a hydrous mineral, the total water content of the basalt decreases.

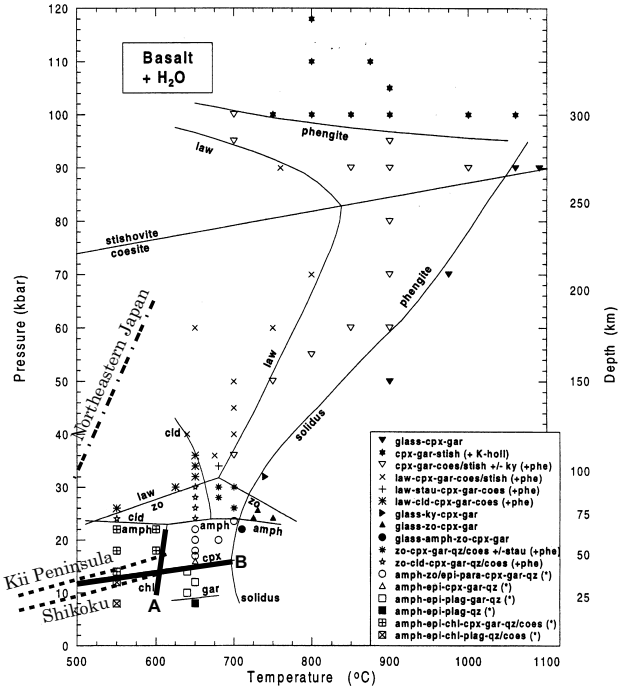

Figure 19: Phase relationships for water-saturated mid-ocean ridge basalt [*Schmidt and Poli*, 1998] and temperature profiles for the upper surfaces of the Pacific Plate under northeastern Japan [*Iwamori*, 1998] and the Philippine Sea Plate beneath the Kii Peninsula and Shikoku [*Hyndman et al.*, 1995] in southwestern Japan: amph = amphibole, chl = chlorite, cld = chloritoid, cpx = jadeitic or omphacitic clinopyroxene, epi = epidote, gar = garnet, law = lawsonite, zo = zoisite. The temperature profile for the Philippine Sea Plate beneath Shikoku crosses a thick line "A" at a depth of about 40km. On the other hand, the temperature profile beneath Kii Peninsula crosses a thick line "B" at similar depth.

Fig. 20 shows Phase diagram for water-saturated average mantle peridotite, modified from a figure by *Schmidt and Poli* (1998), and temperature profiles for the top of the Pacific Plate under northeastern Japan [*Iwamori*, 1998] and the Philippine Sea Plate beneath the Kii Peninsula and Shikoku [*Hyndman et al.*, 1995] in southwestern Japan. Serpentine and some other hydrous minerals including chlorite and amphibole in the mantle peridotite also dehydrate under

the conditions of 600–700°C and 30–50 km. This indicates a possibility that hydrous minerals in the descending mantle wedge along with the slab would also release water. Though, temperature at the top of the mantle wedge beneath Shikoku was estimated at about 450-500°C by *Hyndman et al.* (1995). The temperature is considered too low for serpentine in the mantle wedge to release much of water.

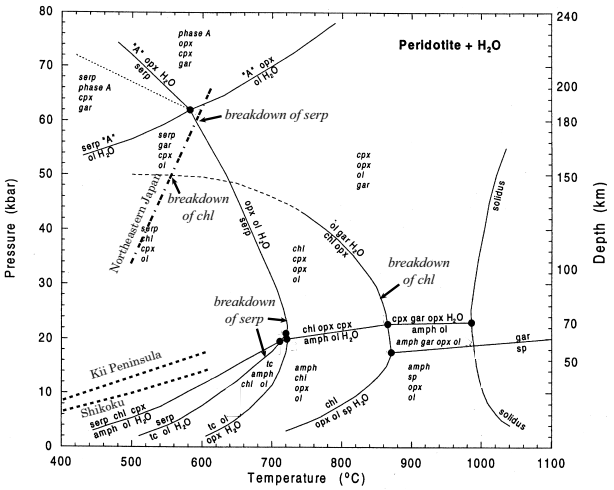

Figure 20: Phase diagram for water-saturated average mantle peridotite, modified from a figure by *Schmidt and Poli* (1998), and temperature profiles for the top of the Pacific Plate under northeastern Japan [*Iwamori*, 1998] and the Philippine Sea Plate beneath the Kii Peninsula and Shikoku [*Hyndman et al.*, 1995] in southwestern Japan: 'A' = phase A, amph = amphibole, chl = chlorite, cpx = clinopyroxene, gar = garnet, ol = olivine, opx = orthopyroxene, serp = serpentine, sp = spinel, tc = talc. The breakdown of serpentine and of chlorite, which mean releasing water, are indicated along the temperature profiles and the phase boundaries.

LFT is observed in the limited range of slab top depth, 25–40 km. Since the amount of water from dehydration processes in the oceanic crust would increase as temperature and pressure increase, a wider belt area would be expected. According to the structure shown by *Kurashimo et al.* (2002), descending oceanic crust starts contact with the mantle wedge under the northern rim of the belt distribution (Fig. 6). Fluid water relating to the tremor would not be supplied to the inland crust in the north of the rim because temperature in the mantle wedge would be low enough for mantle peridotite to absorb ascending water forming hydrous minerals. There would be another possibility that tremor would not occur in the boundary region between the inland crust and the mantle wedge due to a different mechanical condition from that between the inland crust and the oceanic crust.

When the Philippine Sea plate reach at the depth around 50km, melting of the slab would start. On the other hand, the lowest part of the mantle wedge, which consists of hydrous peridotite, descends with slab and release water because of dehydration of serpentine and chlorite at around the depth of 60-80km. At deeper point, the hydrous peridotite starts melting partially. Such high temperature fluid or magma would cause LFE.

Fig. 21 shows schematic view of the process that generates LFT and LFE in the southwest Japan.

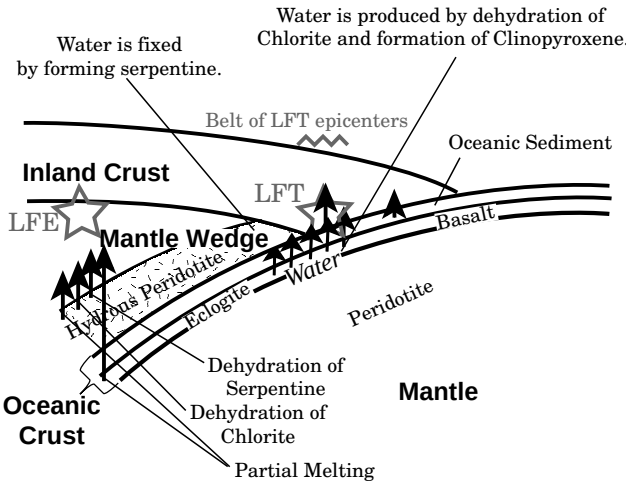

Figure 21: Schematic view of the process that generates LFT and LFE distributed within and of a belt and north of the belt in western Japan. Short arrows show water being released from the descending Philippine Sea Plate. A considerable amount of water is released by both the dehydration of chlorite and the formation of clinopyroxene in slab basalt, and the upwelling water would cause LFT. When the slab comes in contact with the mantle wedge, the upwelling water is fixed as serpentine in the lowest part of the mantle wedge. Therefore, LFT cannot occur because of the absence of fluid. The gray stars show the hypocentral area for LFT and LFE.

Belt LFT activities are not recognized in the east of 138°E line and in Kyushu Island. In addition, a gap is recognized around the Kii channel (Fig. 5). Since the activity is considered to be related to dehydration process of hydrous minerals such as chlorite, the inactive areas would indicate absence of dehydration process due to the following reasons. The Philippine Sea plate moves northwestward in this area [e.g., *Seno et al.*, 1993],

and the plate moves almost along the iso-depth curves of the plate under the channel (Fig. 22). If the dehydration process has almost done around the Kii Peninsula before reaching this area, water would not be supplied. On the other hand, in the area east of 138°E, there are some volcanoes, Mt. Fuji, Mt. Hakone, and so on. Volcanic activities would affect thermal condition and dehydration process of the subducting plate.

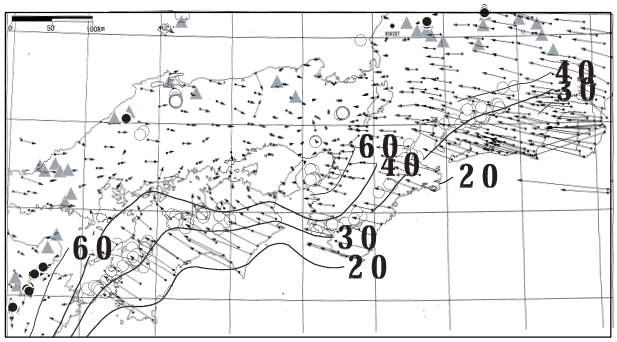

Figure 22: Horizontal displacement vector map based on GPS measurements conducted by the Geographical Survey Institute [*Earthquake Research Committee*, 2001], and depth contours for the Philippine Sea Plate in southwestern Japan. Arrows show horizontal displacement vectors from May in 1997 to June 2000. The fixed station is Fukui. Circles show epicenters of low-frequency events from September 1 in 1999 to February 20 in 2003. Open circles = Low-frequency events far from active volcanoes and the Quaternary volcanoes, Closed circles = Low-frequency events near active volcanoes and the Quaternary volcanoes. Contours are labeled with depth in km.

6 Locating the Tremor with Deconvolution Technique

The JMA determines the source location of the tremor with an ordinary hypocenter determination method based on onset times of enlarging parts of the tremors. With this method, we may miss to detect the tremor with stationary amplitude levels. The unavailability of P-wave onsets makes the locating precision poor. We are developing a tremor-locating method using deconvolution which often used to get receiver functions [e.g., Ammon, 1991].

We get a function of $H(\omega)$ as

$$H(\omega) = \frac{U_j(\omega)U_i^*(\omega)}{\phi(\omega)}G(\omega),$$
$$\phi(\omega) = \max\{U_i(\omega)U_i^*(\omega), cU_i(\omega)U_i^*(\omega)\}$$

where $U_i(\omega)$, $U_j(\omega)$, $G(\omega)$ and c are observed spectra at ith and jth stations, gauss filter [Langston, 1979], and a constant called as water level.

Inverse Fourier-transformed function of $H(\omega)$ should show a peak at a time of arrival-time difference of stations of i and j. Fig. 24 shows examples of the deconvolved functions. The original waveforms are shown in Fig. 23. Some of time series in Fig. 24 show clear peaks. We take times of those peaks to locate the source location.

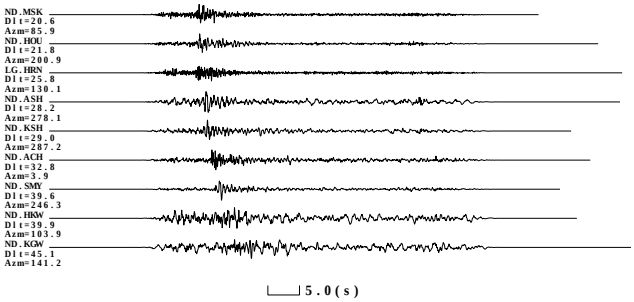

Figure 23: Waveform data used for the deconvolution.

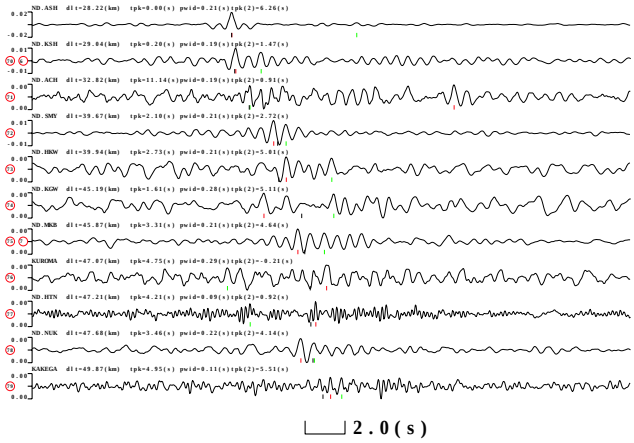

Figure 24: Deconvolved waveforms. The top trace is a result of deconvolution by itself. The primary and secondary peaks are marked by red and green segments.

We determine the source locations as to reduce square of residuals of the arrival-time differences as

$$\sum\{(t_j - t_i)^{obs} - (t_j - t_i)^{cal}\}^2 \to \min.$$

The summation is taken over pairs of arrival-time differences t_i and t_j.

Fig. 25 shows an estimated location (an circle) and iso-arrival-time-difference curves.

7 Conclusions

Unified processing of seismic data in Japan lowered the detectable magnitudes of earthquakes,

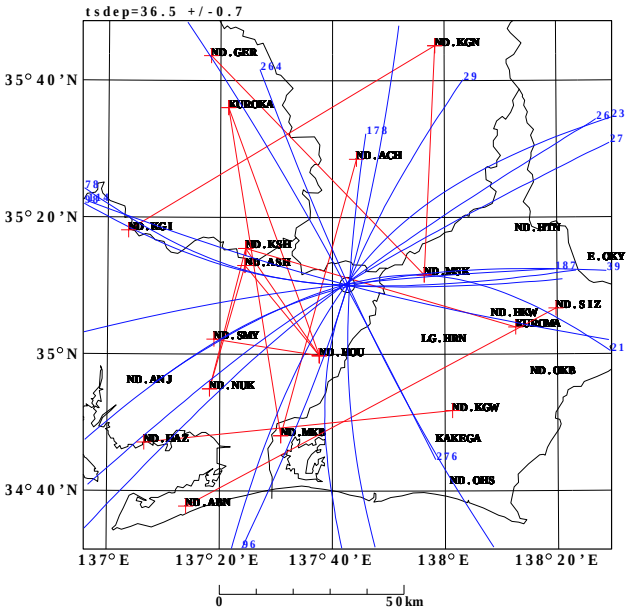

Figure 25: Iso-arrival-time-difference curves. Blue curves, red line segments and a circle show iso-arrival-time-difference curves, the pair of stations, the estimated source location, respectively.

and activities of deep low-frequency earthquakes in non-volcanic regions became recognized. After the development of the Hi-net in southwest Japan, deep tremor of a belt distribution along the strike of the subducting Philippine Sea plate was found.

Source locations of the deep tremors was estimated with onsets of P and S waves, and it was found that source depth ranged from 25 to 40 km and that they were distributed around the boundary region between island and oceanic crusts near mantle wedge.

The east end of the tremor belt distribution is adjacent to the Tokai slow-slip area. The Tokai slow-slip has been continuing since 2000. Activity level of the tremor in the region has been kept high since the beginning of 2003, which coincides with the period of relatively fast slow-slip. The region is located in the west of the probable source area of the Tokai Earthquake. We expect that the tremor activity could be a new valuable indicator for the Tokai Earthquake prediction.

Source force directions inferred from polarization of S-waves were found to be along the direction of the Philippine Sea plate motion, which were clearly different from those of deep low-frequency earthquakes in volcanic regions. The lack of frequency components lower than 0.1 Hz indicates that the tremor is not a direct outcome of the slow slip at the boundary of the Philippine Sea plate.

It is assumed that the tremor is related to water which is produced by dehydration of chlorite and formation of clinopyroxene in the subducting oceanic crust. The northern rim of the belt region seems to correspond to the edge of the mantle wedge. In the north of the edge, fluid water would be depleted to form hydrous minerals such as serpentine in the mantle wedge. This would be the cause of the relatively narrow width of the belt distribution.

Acknowledgments

We used seismic data from the National Research Institute for Earth Science and Disaster Prevention, Hokkaido University, Hirosaki University, Tohoku University, University of Tokyo, Nagoya University, Kyoto University, Kochi University, Kyushu University, Kagoshima University, the National Institute of Advanced Industrial Science and Technology, Tokyo metropolitan government, Shizuoka prefectural government, Kanagawa prefectural government, the City of Yokohama, the Japan Marine Science and Technology Center, and the Japan Meteorological Agency.

References

[1] Ammon, C. J., The isolation of receiver effects from teleseismic P waveforms, *Bull. Seism. Soc. Am., 81*, 2504–2510, 1991.

[2] Aki, K., Scaling law of seismic spectrum, *J. Geophys. Res., 72*, 1217-1231, 1967.

[3] Chouet, B. A, Long-period volcano seismicity: its source and use in eruption forecasting, *Nature, 380*, 309–316, 1996.

[4] Committee for Catalog of Quaternary Volcanoes in Japan, eds., Catalog of Quaternary volcanoes in Japan (CD-ROM with map), The Volcanological Society of Japan, 1999 (in Japanese).

[5] Earthquake Research Committee, On the long-term evaluation of earthquakes in the Nankai trough, 2001 (In Japanese).

[6] Funasaki and Earthquake Prediction Information Division, Revision of the JMA velocity magnitude, *Quart. J. Seism., 67*, 11-17, 2004 (in Japanese with English abstract).

[7] Hasegawa, A. and A. Yamamoto, Deep, low-frequency microearthquakes in or around seismic low-velocity zones beneath active volcanoes in northeastern Japan, *Tectonophysics, 233*, 233-252, 1994.

[8] Hasegawa, A., D. Zhao, S. Hori, A. Yamamoto, and S. Horiuchi, Deep structure of the northeastern Japan arc and its relationship to seismic and volcanic activity, *Nature, 352*, 683-689, 1991.

[9] Hirose, Hi and K. Obara, Repeating slow slip events which correlate deep low-frequency tremor activity in Southwest Japan, *Prog. Abstr. Fall Meeting Seismol. Soc. Jpn.*, C098, 2003 (in Japanese).

[10] Hyndman, R. D., K. Wang, and M. Yamano, Thermal constraints on the seismogenic portion of the southwestern Japan subduction thrust, *J. Geophys. Res., 100*, 15373–15392, 1995.

[11] Iwamori, H., Transportation of H_2O and melting in subduction zones, *Earth Planet. Sci. Lett., 160*, 65–80.

[12] Katsumata, A., Revision of the JMA displacement magnitude, *Quart. J. Seism., 67*, 1-10, 2004 (in Japanese with English abstract).

[13] Kamaya, N. and A. Katsumata, Low-frequency events away from volcanoes in the Japan Islands, *Zisin 2, 57*, 11–28, 2004 (in Japanese with English abstract).

[14] Katsumata, A. and N. Kamaya, Low-frequency continuous tremor around the Moho discontinuity away from volcanoes in the southwest Japan, *Geophys. Res. Lett., 30*, 1, 10.1029/2002GL015981, 2003.

[15] Kurashimo, E., M. Tokunaga, N. Hirata, T. Iwasaki, S. Kodaira, Y. Kaneda, K. Ito, R. Nishida, S. Kimura, and T. Ikawa, Geometry of the subducting Philippine Sea plate and the crustal and upper mantle structure beneath eastern Shikoku Island revealed by seismic refraction/wide-angle reflection profiling, *Zisin 2, 54*, 489–505, 2002 (in Japanese with English abstract).

[16] Langston, C. A., Structure under Mount Rainier, Washington, inferred from teleseismic body waves, *J. Geophys. Res., 84*, 4749-4762, 1979.

[17] Nishide, N., T. Hashimoto, J. Funasaki, H. Nakazawa, M. Oka, H. Ueno, N. Yamada, I. Sasakawa, K. Maeda, K. Sugimoto, and T. Takashima, Nationwide activity of low-frequency earthquakes in the lower crust in Japan, *Abstr. Jpn. Earth and Planet. Sci. Joint Meeting*, sk-p002, 2000.

[18] Obara, K., Nonvolcanic deep tremor associated with subduction in southwest Japan, *Science, 296*, 1679–1681, 2002.

[19] Okada, Y., K. Kasahara, S. Hori, K. Obara, and S. Aoi, Hi-net (1): outline, *Prog. Abstr. Fall Meeting Seismol. Soc. Jpn.*, P004, 2000 (in Japanese).

[20] Tsuboi, C., Determination of the Gutenberg-Richter's magnitude of earthquakes occurring in and near Japan, *Zisin 2, 7*, 185–193, 1954 (In Japanese with English abstract).

[21] Schmidt, M. W. and S. Poli, Experimentally based water budgets for dehydrating slabs and consequences for arc magma generation, *Earth Planet. Sci. Lett., 163*, 361–379, 1998.

[22] Seno, T., S. Stein, and A. E. Gripp, A model for the motion of the Philippine Sea plate consistent with NUVEL-1 and geological data, *J. Geophys. Res., 98*, 17941–17948, 1993.

[23] Ukawa, M. and K. Obara, Low frequency earthquakes around Moho beneath the volcanic front in the Kanto district, central Japan, *Bull. Volcanol. Soc. Japan, 38*, 187–197, 1993 (in Japanese with English abstract).

[24] Ukawa, M. and K. Ohtake, A monochromatic earthquake suggesting deep-seated magmatic activity beneath the Izu-Ooshinma volcano, Japan, *J. of Geophys. Res., 92*, 12,649–12,663, 1987.